Journal of Materials and Engineering Structures

Research Paper

Evaluation of loading capacity of corroded reinforced concrete beams using experiment and finite element method

Thanh-Hung Nguyen [a], Manh-Hien Nghiem [b], Duy-Duan Nguyen [c,*]

[a] *Faculty of Civil Engineering, HCMC University of Technology and Education, HCMC, Vietnam*

[b] *College of Engineering & Applied Science, University of Colorado Denver, CO 80217, USA*

[c] *Department of Civil Engineering, Vinh University, Vinh 461010, Vietnam*

ARTICLE INFO

Article history:

Received : 15 July 2020

Revised : 23 August 2020

Accepted : 28 August 2020

Keywords:

Corrosion effect

Reinforced concrete beam

Finite element model

Experiment

ABSTRACT

The purpose of this paper is to evaluate the performance of corroded reinforced concrete (RC) beams using experiments and a proposed finite element (FE) model, which is able to consider the reduction of the reinforcement diameter and adhesion force. The developed FE model comprised of three main components including concrete elements, reinforcing bar elements, and adhesion elements, in which the plane cross-section hypothesis was adopted. Thus, the necessary number of elements in the model of corroded RC beam was greatly reduced, while the accuracy of the model was still ensured. An experimental test was employed to verify the developed FE model. The results show that the proposed FE model in this study is capable of modeling RC beams under corrosion effects. Additionally, the rebar diameter and adhesion force have a significant influence on the load-carrying capacity of corroded RC beams. Moreover, a series of experimental tests of corrosive RC beams including 1-month, 2-month, and 3-month corrosion levels was conducted for various exposed times to investigate the influences of the corrosion time on the strength of RC beams. It reveals that the effect of the corrosion time on the strength of RC beams show to be pronounced.

1 Introduction

The calculation of the reinforced concrete (RC) structures for the current design problems is quite fully provided by design standards. However, the load carrying capacity of RC structures has been reduced with time due to several reasons. Thus, accurate evaluation of the current state of RC structures, which have been degraded after use, is necessary.

The effect of corrosion of reinforcement in concrete on the bearing capacity of RC structures has been numerously investigated. Rodriguez et al. [1] conducted a series of experimental tests for studying the failure mechanisms of the corroded RC beams. Vidal et al. [2] provided relationships between the distributions of rebar corrosion and the wide of cracks of RC beams using experimental tests. Numerical and experimental studies on the assessment of the impact resistance of corroded

* *Corresponding author,*
E-mail address: duyduankxd@vinhuni.edu.vn

e-ISSN: 2170-127X,

RESEARCH REVIEW of Sciences and Technologies

RC beams were performed by Lu et al. [3]. Han et al. [4] and Malumbela et al. [5] carried out a set of tests to investigate the influences of longitudinal rebar corrosion on the shear capacity of RC beams. In the study of Zhu et al. [6], they investigated the behaviour of 26-year corroded RC beams, in which the load-deflection curves, corrosion maps, and the loss are of reinforcements were observed. Kearsley and Joyce [7] evaluated the effect of corrosion product on the bond strength and flexural strength of RC slabs. The application of finite element method to analyse the performance of corroded RC structures by using commercial programs such as ANSYS, DIANA, and ATENA has also provided good results compared with those in experiments [8-13].Previous studies mostly dealt with specific cases and used commercial finite element software for modelling corroded structures and comparing with experimental results. However, a challenge in calculation will be raised since input parameters including concrete strength, cohesion force between steel and concrete, and the reduction of diameter of reinforcing bars are considered as random parameters. The calculated simulation with hundreds of investigated cases will be time-consuming with existing FE software. Therefore, a proposed algorithm and developed software are needed for speeding up the calculation effort in simulations of corroded RC beams with random input parameters. Additionally, the influence of corrosion time on loading capacity of corroded RC beams is not considered sufficiently.

In this paper, a FE model of corroded RC beams was developed considering the reduction of reinforcement diameter and adhesion force. The model composed of three main components including concrete elements, steel rebar elements, and adhesion elements were built based on the plane cross-section hypothesis. Thus, the necessary number of elements in the model of corroded RC beam was greatly reduced while the accuracy of the model was still ensured. The FE analysis results were also compared with those of experimental tests. The comparisons showed that the algorithm and program built for FE model could provide accurate and reliable results in calculation of corroded RC beams. The effect of the reduction of the bonded strength between reinforcement and concrete as well as the reduction of steel rebar diameter on load carrying capacity of corroded RC beam was then evaluated. Additionally, a series of experiments are performed for different beams with various corrosion levels to investigate the effect of corrosion time on the strength of RC beams.

2 FE model for loading capacity evaluation of corroded RC beams

2.1 Material models

The material model of concrete used in this study is presented in Fig. 1. The stress-strain curve of the concrete in compression is modelled into 2 main parts (Fig. 1a): the first part is linear elastic initiates from 0 to the largest compressive stress f_{cc}; and the second part is horizontal plastic.

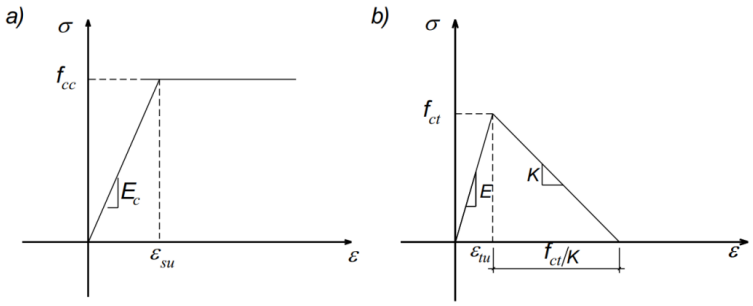

Fig. 1 –Concrete model: (a) compression and (b) tension

The concrete model in compression can be expressed as follows.

$$\sigma = E_c\varepsilon \text{if} \varepsilon \le \varepsilon_{su} \text{ and } \sigma = f_{cc} \text{if} \varepsilon > \varepsilon_{su} \quad (1)$$

The stress-strain curve of the concrete in tension is also modelled into 2 main parts (Fig. 1b): the first part is linear lactic initiates from 0 to the largest tensile stress f_{ct}, where the tensile elastic modulus equals to the compressive elastic modulus; and the second part is a straight line represented by attenuation stress module *K*. The concrete model in tension can be expressed as follows.

$$\sigma = E\varepsilon \text{ if } \varepsilon \le \varepsilon_{tu}$$

$$\sigma = f_{ct} - (\varepsilon - \varepsilon_{tu})K \text{ if } \varepsilon_{tu} < \varepsilon < \varepsilon_{tu} + \frac{f_{ct}}{K} \tag{2}$$

$$\sigma = 0 \text{ if } \varepsilon \geq \varepsilon_{tu} + \frac{f_{ct}}{K}$$

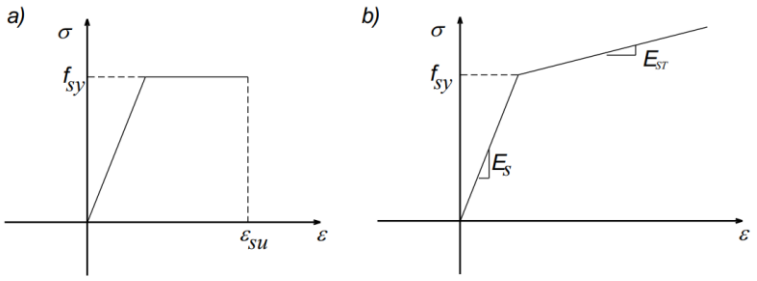

Fig. 2–Material models of reinforcement: (a) elasto-plastic model and (b) bilinear model

A linear elastic – perfectly plastic model for reinforcement is presented in Fig. 2a while a bi-linear elasto-plastic model for reinforcement is illustrated in Fig. 2b. Rodriguez et al. [1] used the bi-linear elasto-plastic model with elastic modulus of the linear hardening part of $E_{ST} = E_S / 250$. The yield strength f_{sy} and elastic modulus E_S of steel reinforcement are provided in standards. The stress-strain curves of steel reinforcement are considered to be the same in both tension and compression. The material model presented in Fig. 2b is used in this study.

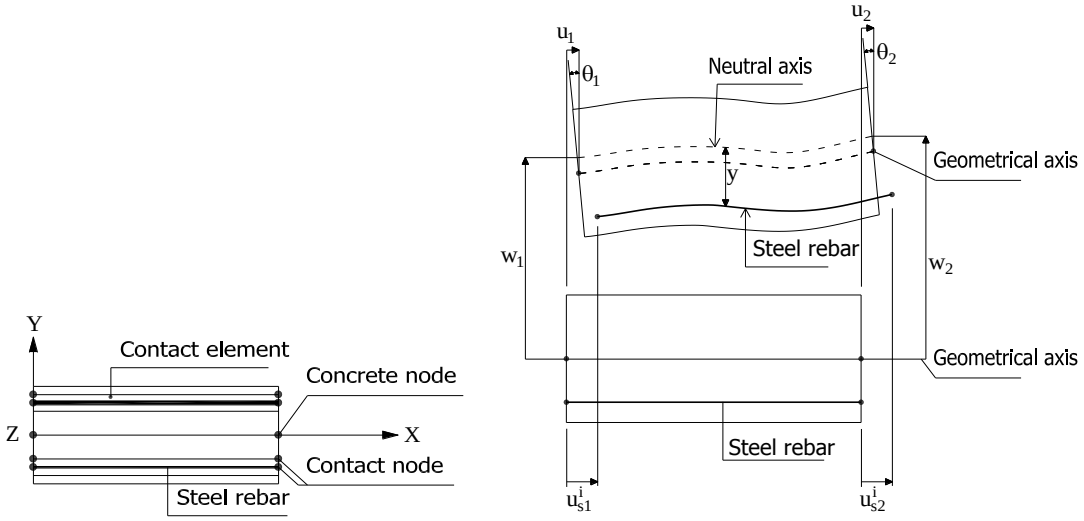

Fig. 3–RC beam element

2.2 FE formulation of corroded RC beam

Corroded RC beam element considering adhesion force consists of 3 element types illustrated in Fig. 3, as follows: (a) concrete element; (b) reinforcement element; and (c) contact element. There are multiple nodes at each end of RC element:

- The nodes that connect the concrete element and the contact element have three degrees of freedom including displacement along *X* and *Y* axes and rotation around *Z* axis.
- The nodes that connect the contact element and the reinforcement element have one degree of freedom: displacement along *X* axis.

According to FE method, the displacements at any points on the axis of the beams are approximately equal to the displacement of the node. The shape functions and deformation matrix of each element type are established below.

2.2.1 Concrete element

The concrete element has two nodes, as shown in Fig. 4(a), where each node has three degrees of free dom including axial displacement along *X* and *Y* and rotation around*Z* axis. The displacement*u* along*X* axis can beapproximated as [14],

$$u = N_{u_1} u_1 + N_{u_2} u_2 \tag{3}$$

whereu_1 and u_2 are the displacements at node 1 and 2, respectively; N_{u_1} and N_{u_2} are the shape functions, given by

$$N_{u_1} = 1 - x/L \text{and } N_{u_2} = x/L \tag{4}$$

The axial deformation matrix of concrete element is

$$[B_{cu}] = \left[\frac{dN_{u_1}}{dx} \frac{dN_{u_2}}{dx}\right] \tag{5}$$

The horizontal displacement *w* of the element along the *Y* axis can be approximated as

$$w = N_{w_1} w_1 + N_{w_2} \theta_1 + N_{w_3} w_2 + N_{w_4} \theta_2 \tag{6}$$

where w_1 and w_2 are the horizontal displacement at node 1 and 2, respectively; θ_1 and θ_2 are the rotated angle around *Z* axis at node 1 and 2, respectively; and N_{w_1}, N_{w_2}, N_{w_3} and N_{w_4} are the Hermite shape functions.

The bending deformation matrix of concrete element can be determined as

$$[B_{cw}] = \left[\frac{d^2 N_{w_1}}{dx^2} \frac{d^2 N_{w_2}}{dx^2} \frac{d^2 N_{w_3}}{dx^2} \frac{d^2 N_{w_4}}{dx^2}\right] \tag{7}$$

2.2.2 Reinforcement element

Reinforcement element has only displacement along *X* axis as shown in Fig. 4(b). Since this element connects to the concrete element through the adhesion element, the displacement of this element depends on the displacement of concrete and adhesion elements. The relative displacement between reinforcement and concrete or displacement of the adhesion element can be approximated as follows.

$$\Delta_i = N_{\Delta_1} \Delta_{i_1} + N_{\Delta_2} \Delta_{i_2} \tag{8}$$

where N_{Δ_1} and N_{Δ_2} are the shape functions $N_{\Delta_1} = 1 - x/L$; $N_{\Delta_2} = x/L$ $N_{\Delta_1} = 1 - x/L$; $N_{\Delta_2} = x/L$.

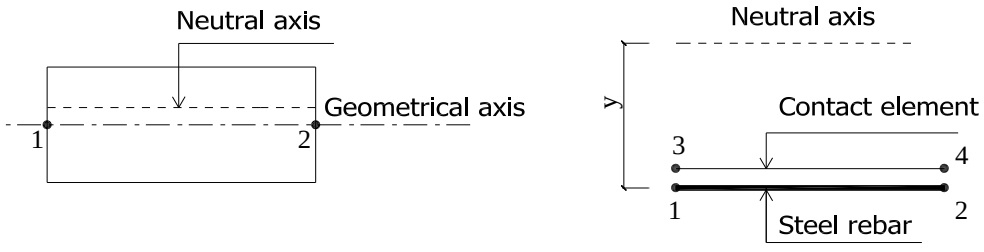

(a) concrete (a) reinforcement

Fig. 4–Concrete and reinforcing bar elements

Denoted $y_i$as the distance from the neutral axis to the i^{th} reinforcement, based on the plane cross-section hypothesis, the displacement at any point in the i^{th} reinforcement can be expressed as

$$u_S = u - y_i \frac{dw}{dx} - \Delta_i \tag{9}$$

Eq. (9) can be written as a function of nodal displacements, as follows

$$u_s = N_{u_1}u_1 + N_{u_2}u_2 - y_i\left(N'_{w_1}w_1 + N'_{w_2}\theta_1 + N'_{w_3}w_2 + N'_{w_4}\theta_2\right) - N_{\Delta_1}\Delta_{i_1} - N_{\Delta_2}\Delta_{i_2} \tag{10}$$

Denoted u_{s_1} and u_{s_2} as the displacement of reinforcement at node 1 and 2, respectively, the number of displacements in *n* reinforcement bars is 2*n*. From Eq. (9), u_{s_1} and u_{s_2} can be expressed as

$$\begin{aligned} u_{s_1} &= u_1 - y_i\theta_1 - \Delta_{i_1} \\ \text{thus, } \Delta_{i_1} &= u_1 - y_i\theta_1 - u_{s_1} \end{aligned} \tag{11}$$

$$\begin{aligned} u_{s_2} &= u_2 - y_i\theta_2 - \Delta_{i_2} \\ \text{thus, } \Delta_{i_2} &= u_2 - y_i\theta_2 - u_{s_2} \end{aligned} \tag{12}$$

Substituting Eqs. (11) and (12) into Eq. (10), becomes

$$u_s = N_{s_1}w_1 + N_{s_2}\theta_1 + N_{s_3}w_2 + N_{s_4}\theta_2 + N_{s_5}u_{s_1} + N_{s_6}u_{s_2} \tag{13}$$

where $N_{s_1}, N_{s_2}, N_{s_3}, N_{s_4}, N_{s_5}, N_{s_6}$ are the shape functions of reinforcement element. The deformation of the reinforcement then can be written as

$$\varepsilon_s = \frac{du_s}{dx} = [B_s]\left[w_1\theta_1 w_2\theta_2 u_{s_1} u_{s_2}\right]^T \tag{14}$$

where $[B_s]$ is the deformation matrix of reinforcement element, which is expressed as follows.

$$[B_s] = \left[\frac{dN_{s_1}}{dx}\frac{dN_{s_2}}{dx}\frac{dN_{s_3}}{dx}\frac{dN_{s_4}}{dx}\frac{dN_{s_5}}{dx}\frac{dN_{s_6}}{dx}\right] \tag{15}$$

2.2.3 Adhesion element between concrete and reinforcement

The model for adhesion element between concrete and reinforcement is illustrated in Fig. 5. From Eqs. (8), (11), and (12), the relative displacement can be expressed as

$$\Delta_i = N_{\Delta_1}\left(u_1 - y_i\theta_1 - u_{s_1}\right) + \mathrm{N}_{\Delta_2}\left(u_2 - y_i\theta_2 - u_{s_2}\right) \tag{16}$$

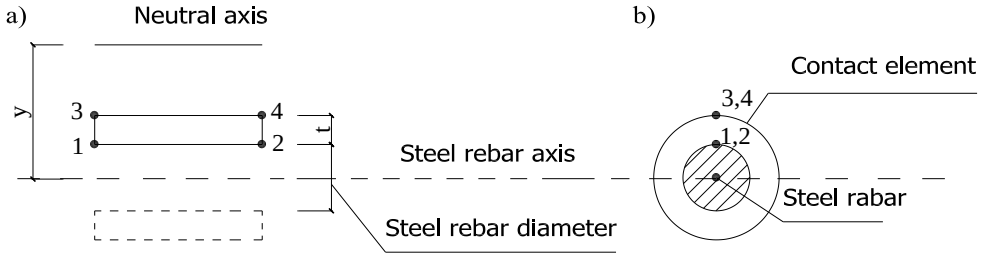

Fig. 5–Contact element: (a) Longitudinal section; (b) Cross-section

Assuming the thickness of the adhesion element i^{th} is *t*, the shear strain of the adhesion i^{th} can be written as the following form:

$$\begin{aligned} \gamma_i = \frac{\Delta_i}{t} &= \frac{1}{t}\left[N_{\Delta_1}\left(u_1 - y_i\theta_1 - u_{s_1}\right) + N_{\Delta_2}\left(u_2 - y_i\theta_2 - u_{s_2}\right)\right] \\ &= [B_{cont}]\left[u_{s_1}u_1 w_1\theta_1 u_{s_2}u_2 w_2\theta_2\right]^{\mathrm{T}} \end{aligned} \tag{17}$$

where $[B_{cont}]$ is the deformation matrix of adhesion element, which is expressed as

$$[B_{cont}] = \gamma_i = \left[-\frac{N_{\Delta_1}}{t}\frac{N_{\Delta_1}}{t} \;\; 0 \;\; -\frac{N_{\Delta_1}}{t}y_i \;\; -\frac{N_{\Delta_2}}{t}\frac{N_{\Delta_2}}{t} \;\; 0 \;\; -\frac{N_{\Delta_2}}{t}y_i\right] \tag{18}$$

Here, we have defined the shape functions and deformation matrixes of the concrete element, reinforcement element, and adhesion element of the RC beam element. The nodal displacements of the RC beam element consist of longitudinal displacement *u*, horizontal displacement *w*, and rotation angle θ of the concrete element and the longitudinal displacement of reinforcement u_{si}, where the number of unknown u_{si} depends on the number of reinforcement bars in the beams.

2.2.4 Equilibrium equation and solution method

Substituting the displacement and deformation equations into equilibrium, Eq. (9) becomes

$$\delta\Pi_{eq} = \delta\tilde{u}^T\left[\int_{V_e} B^T\sigma dV - \int_{V_e} N^T b dV - \int_{S_e} N^T\bar{t}dS\right] \tag{19}$$

Taking the sumover the object domain and due to the random$\delta\tilde{u}$, we obtain the static equilibrium equation for small deformation problem and nonlinear physics as

$$P(\sigma) = f \tag{20}$$

During the nonlinear structural analysis, the nonlinear relationship is linearized and the load is divided into small steps. Currently, the most used methods for solving nonlinear equations are Newton-Raphson and improved New-Raphson. Here, we use the improved Newton-Raphson method, which uses the initial stiffness matrix K_I in each loop instead of using the tangential stiffness matrix K_T. Therefore, the greater number of loops is required to achieve the necessary convergence.

2.2.5 Determination of stress in the elements

The beam curvature is determined through the rotation angle as the following equation

$$\phi = \frac{d\theta}{dx} \tag{21}$$

While, the beam shear is calculated from the moments M_1 and M_2 at the ends of the beam as

$$Q_1 = -Q_2 = \frac{M_2 - M_1}{L} \tag{22}$$

where *L* is the length of the beam. The moment in the beam can be determined by dividing the cross section of the beam into fibers along the y axis direction, as illustrated in Fig. 6 [15].

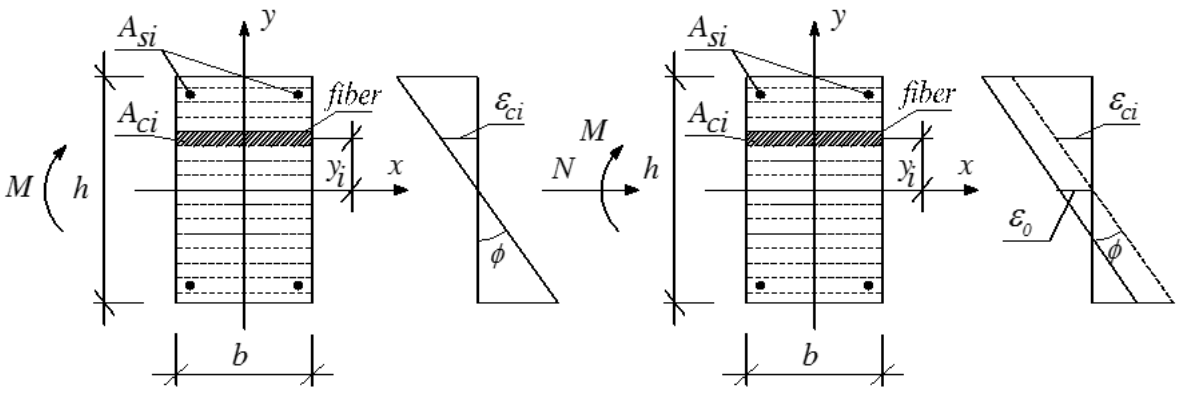

Fig. 6–Split cross section of reinforcement bar into fibers

The axial force *N* and moment *M* at cross section are determined as

$$N = \sum_{i=1}^{n_c} A_{ci}.\sigma_{ci}\ ; M = \sum_{i=1}^{n_c} A_{ci}.\sigma_{ci}\ .y_i \tag{23}$$

From Eq. (14), the stress in the reinforcement can be computed as

$$\sigma_s = E_s\varepsilon_s = E_s[B]\left[w_1\theta_1 w_2\theta_2 u_{s_1} u_{s_2}\right]^T \tag{24}$$

Since the stress distributed along the reinforcement bar does not comply with any certain function, it is assumed to be a linear distribution as follows

$$\sigma_s = \sigma_{s_1} + \frac{\sigma_{s_2} - \sigma_{s_1}}{L} x \tag{25}$$

where$\sigma_{s_1}$and $\sigma_{s_2}$are the stress at the beginning and the end of the element (Fig. 3).

Similar to reinforcement bar, stress distributed along the adhesion element does not comply with any certain function, it is assumed to be a linear distribution as follows.

$$\tau_s = \tau_{s_1} + \frac{\tau_{s_2} - \tau_{s_1}}{L} x \tag{26}$$

2.2.6 Corrosion model of reinforcement in concrete

The most obvious result of reinforcement steel corrosion is the reduction of the cross-section area. Since the evaluation of the corrosion of reinforcement in existent structures is a rather difficult task, the corrosion of reinforcement bars can be considered as averaged results. The adhesion between the reinforcement and concrete depends on several factors such as the level of covered concrete, anchors, and cracks in which the ratio of the covered concrete layer and the diameter of reinforcement bar is usually chosen as the representative characteristic of close bond between rebar and concrete. Fig. 7 illustrates a diagram of adhesion force $\tau$of reinforcement versus the slip *s*, which was established based on the experimental results [16,17].

2.3 Proposed algorithm

Based on the presented FE formulation, a practical program for evaluating capacity of corroded RC beams called CBS was developed using Delphi programming language [18]. During the calculation, the load acting on the beam was gradually increased until the stresses in tensile reinforcement were fully plastic, this state is corresponded to the plastic failure. Fig. 8 schematically shows the algorithm of the program.

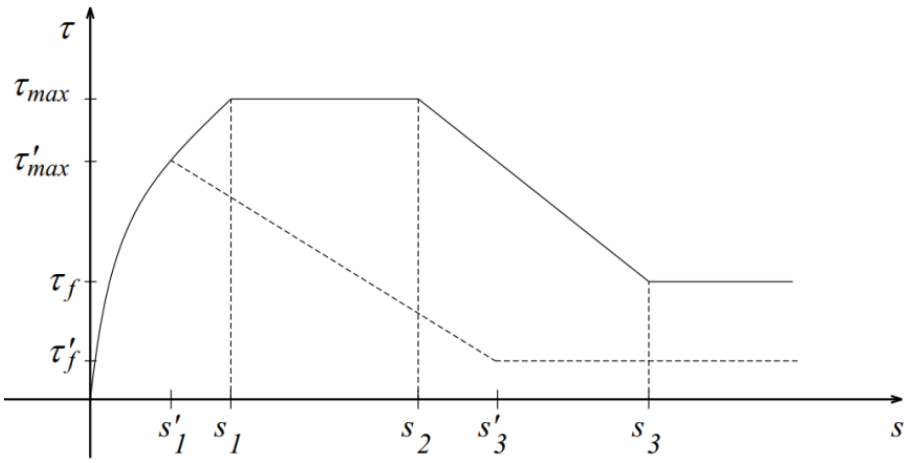

Fig. 7– Bond-slip diagram for monotonic loading [8]

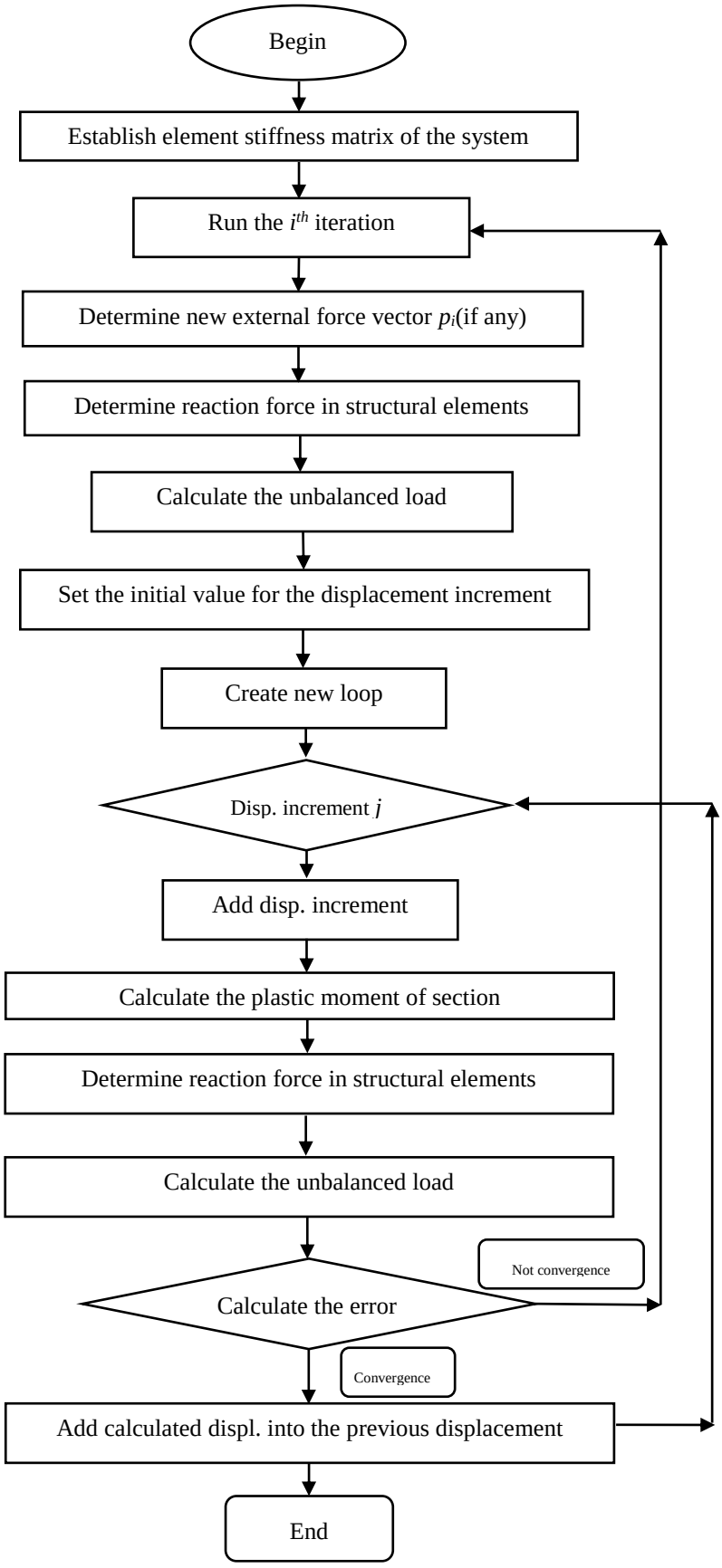

Fig. 8–Algorithm for CBS program

3 Validation of FE model

The corroded RC beam in the experiment of Rodriguez et al. [1] is employed to simulate in the developed program, as shown in Fig. 9. The authors empirically studied the extend of corrosion of the steel reinforcement in a RC beam with the length of l = 2300 mm, the depth of h = 200 mm, and the width of b = 150 mm. The concentrated load P is applied at the points with a distance of 800 mm to the supports. Two reinforcing bars with ϕ10 wereplaced at the bottom, while two reinforcement ϕ8 were installed at the top of the beam section. The stirrups with ϕ6were also installed. The compressive strength of concrete is varied in the range from 34 MPa to 50 MPa. Two beams with identical dimensions, namely D115 and D111 were tested to account for with and without corrosion effects, respectively. The reinforcement in each RC beam was assumed to be corroded with different levels to ensure the designed corrosion, in which the beam D111 had no corrosion while the beam D115 was corroded 6.7%.

Since the experiment just provided only strength of concrete and steel reinforcement, other material properties used in FE simulations were determined based on other information sources or the previous experience. The material parameters used in this study are shown in Tables 1 and 2 [8].

Table 1 - Concrete properties

Property	Notation	D111	D115	Remark
Compressive strength	f_{cc}	50 MPa	31.4 MPa	Sæther and Sand [8]
Tensile strength	f_{ct}	3.5 MPa	2.8 MPa	Sæther and Sand [8]
Elastic modulus	E_c	32,200 MPa	28,300 MPa	Sæther and Sand [8]
Poisson's ratio	v_c	0.2	0.2	Assumption
Shear coefficient	β	0.1	0.1	Assumption
Reduced modulus	K	5,123 MPa	5,122 MPa	CBS
Adhesion force	τ_{max}	7.0 MPa	4.55 MPa	Prediction

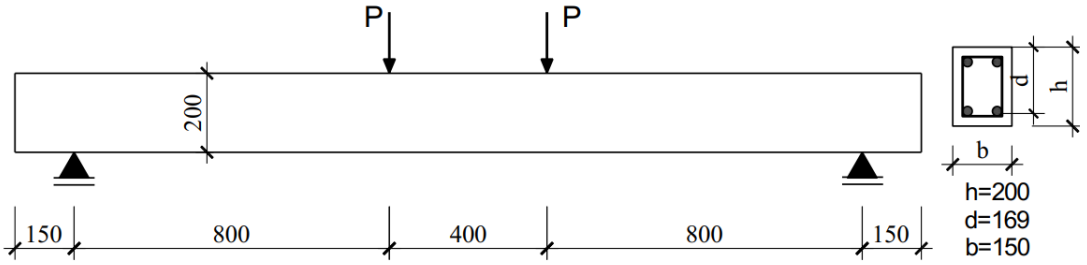

(a) Dimensions of the beam and applied loading

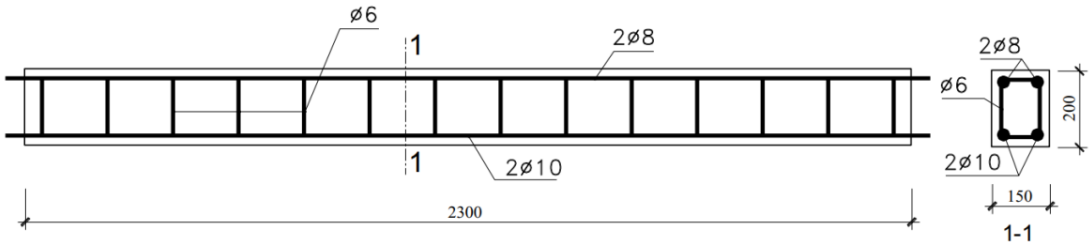

(b) Reinforcement details

Fig. 9–RC beam used in experiments of Rodriguez et al. [1]

Fig. 10 shows the finite element model of RC beam in CBS program. The beam was divided into 27 small elements, in which the supported points (indicating in pink circles) are located at the end of elements #1 and #27, whereas the loaded points (indicating in pink lines) are at the end of elements #11 and #17. The blue lines are represented reinforcing bar elements. Bothe the uncorroded and corroded beams were tested under static loading until failure. The vertical load was increased from 5 kN to 40 kN for uncorroded beam (i.e. D111) and from 5 kN to 30 kN for the beam with corrosion (i.e. D115).

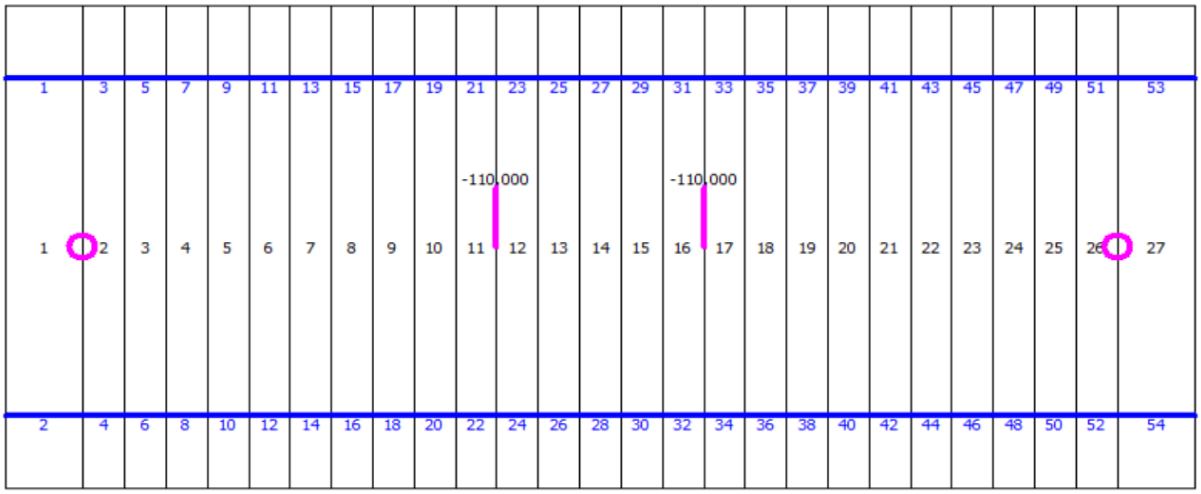

Fig. 10–FE model of RC beam in CBS software

Table 2 - Reinforcing bar properties

Property	Notation	Value	Remark
Yield strength	f_{sy}	ϕ_{10}: 575 MPa	Sæther and Sand [8]
		ϕ_8: 615 MPa	
		ϕ_6: 626 MPa	
Ultimate strength	f_{su}	ϕ_{10}: 655 MPa	
		ϕ_8: 673 MPa	
		ϕ_6: 760 MPa	
Elastic modulus	E_s	206,000 MPa	Assumption
Shear modulus	E_{ST}	824 MPa	Assumption

Fig. 11 shows the comparison of load-displacement curves at the midspan section of the uncorroded and corroded RC beams between the results obtained by CBS program and experimental results as well as others FE software including ATENA and ANSYS. The relatively good comparison indicates that CBS program provides reliable results even though a tolerance is existing.

Figs. 12 and 13 show the distribution of stresses in reinforcing bars and adhesive forces between concrete and reinforcing bars of the beam, respectively. It can be observed that a large stress of the reinforcements is focused on the mid span area of the beam. This trend is also similar to the distribution of adhesive forces between concrete and steels, however, it is distributed in a zigzag shape because of heterogeneous interface between concrete and steels along the beam. Fig. 14 illustrates the cracks of beams D111 and D115 at the final stage of loading.

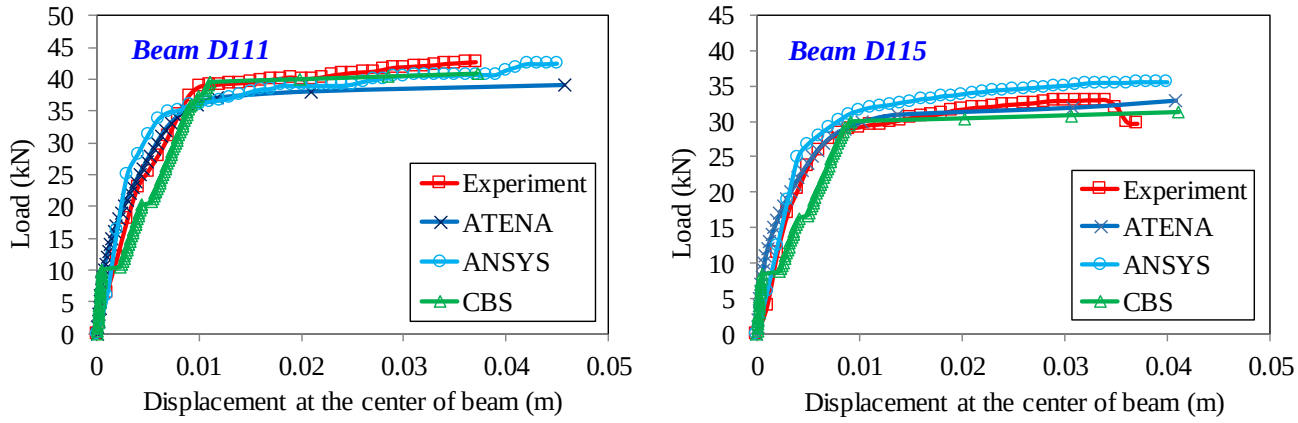

(a) Beam D111 (b) Beam D115

Fig. 11–Load versus central deflection for the reference beams

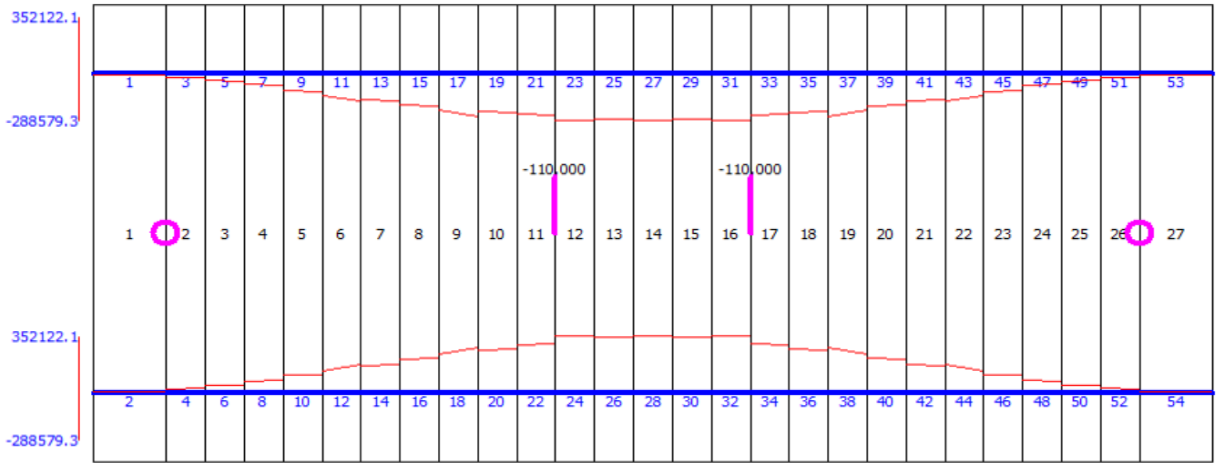

Fig. 12(a)– Stress distribution in reinforcing bars in CBS program (unit: KPa) for Beam D111

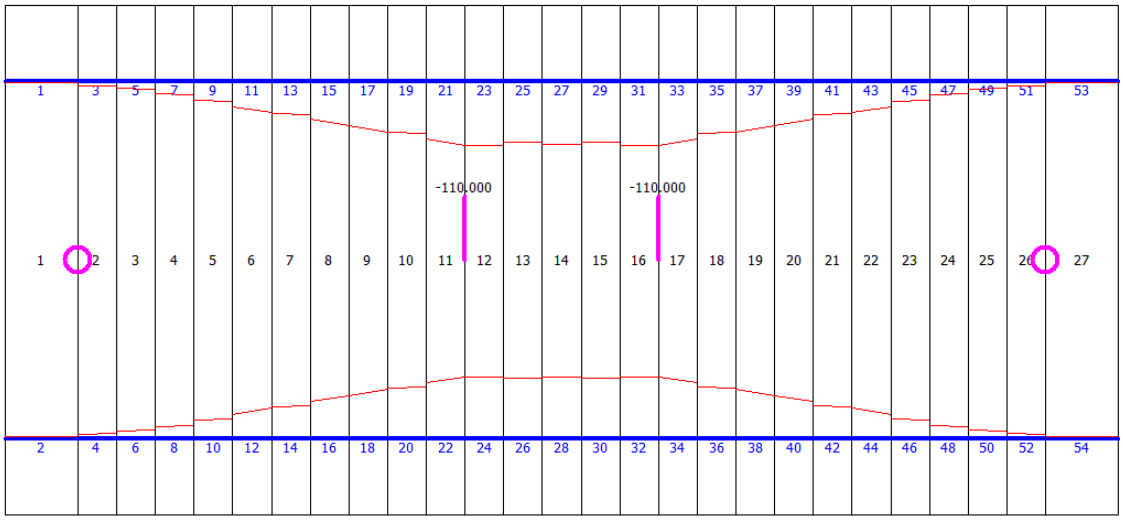

Fig. 12(b)– Stress distribution in reinforcing bars in CBS program (unit: KPa) for Beam D115

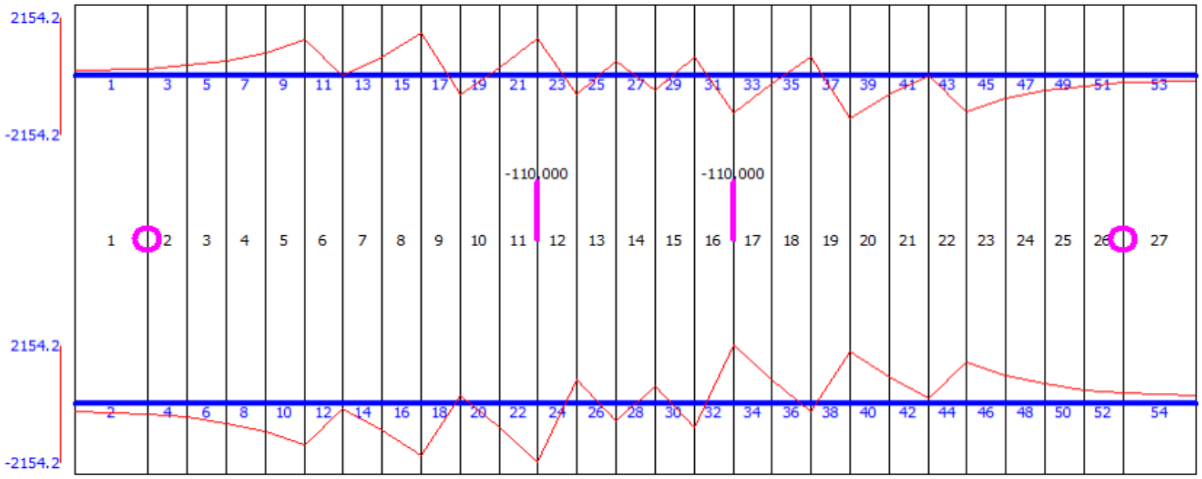

Fig. 13(a)– Adhesion forces between concrete and reinforcing bars in CBS program (unit: KPa) for Beam D111

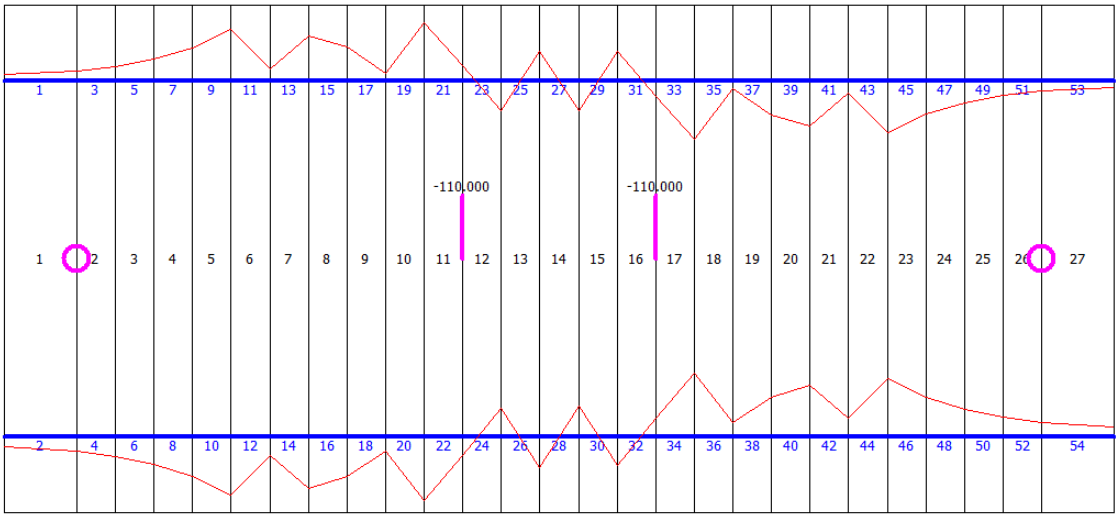

Fig. 13(b)– Adhesion forces between concrete and reinforcing bars in CBS program (unit: KPa) for Beam D115

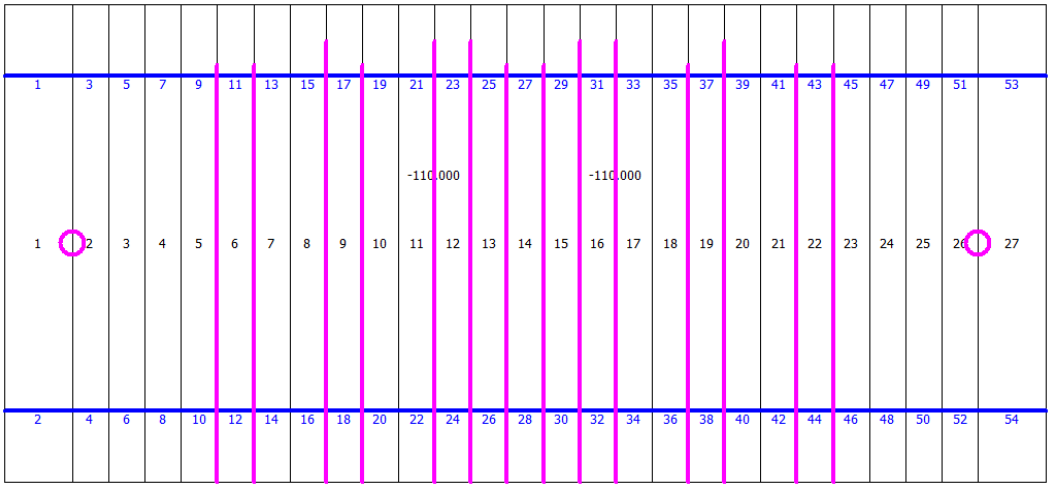

Fig. 14(a)– Cracks of Beam D111 in CBS program for

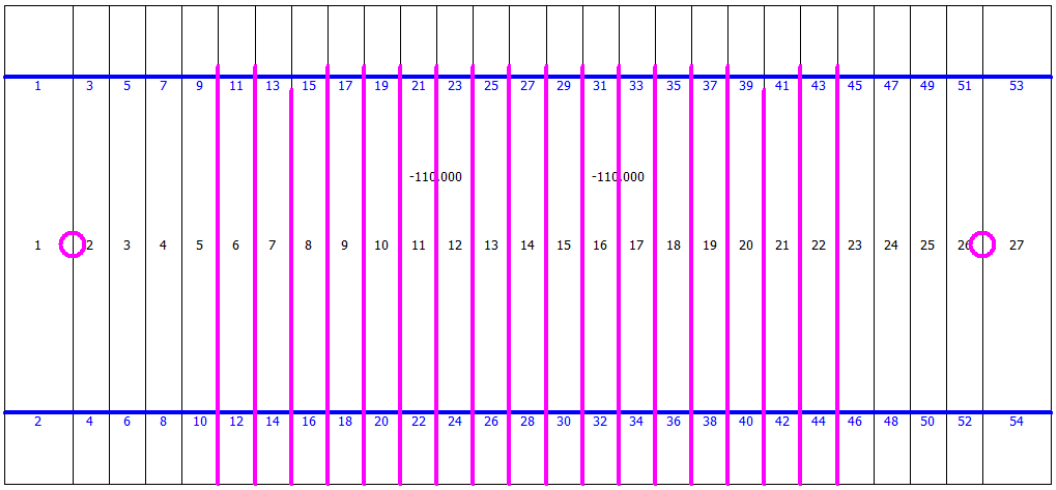

Fig. 14(b)– Cracks of Beam D115 in CBS program for

4 Parametric study

4.1 Effect of the reduction of reinforcing bar diameter

The effect of corrosive level on the structural performance of the beam is investigated in this study. A variation of diameter of reinforcing bars, which is represented for corrosion level, was considered to investigate the change of load-deflection relationship of the beam. Fig. 15 shows the behaviour of the beam D115 with the reduction of reinforcing bar diameter performed in CBS program. It can be observed that stiffness and ultimate strength of the beam was gradually reduced from the diameter reduction of 3% to 15%.

4.2 Effect of the reduction of adhesion between concrete and reinforcing bars

The effect of adhesion between concrete and reinforcing bars was also examined in this paper. Fig. 16 shows the load-deflection curves for a variation of adhesive forces. The initial stiffness of the beam was not changed until the loading induced a deflection about 0.01 m. However, the adhesion has a significant influence on the ultimate strength of the beam. It is also shown in Fig. 16 that the strength of the beam was increased from 34 kN to 40 kN corresponding to the adhesion force increased from 4.5 MPa to 7.0 MPa, respectively.

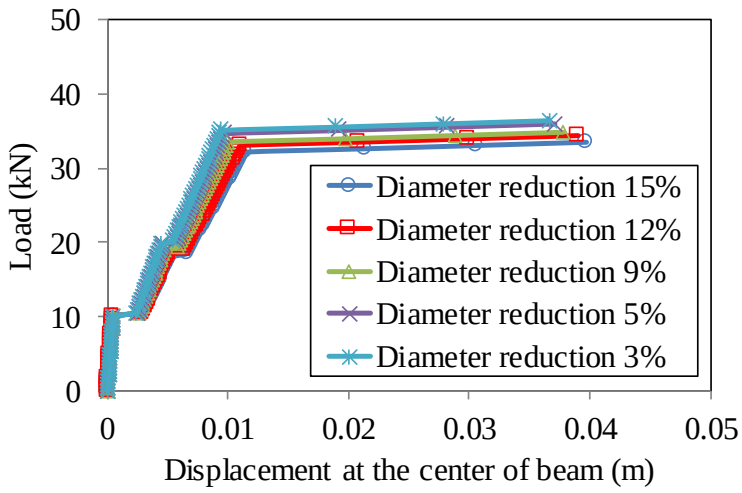

Fig. 15–Load-displacement relationship of the beam D115 with various reduction of the reinforcing bar diameter

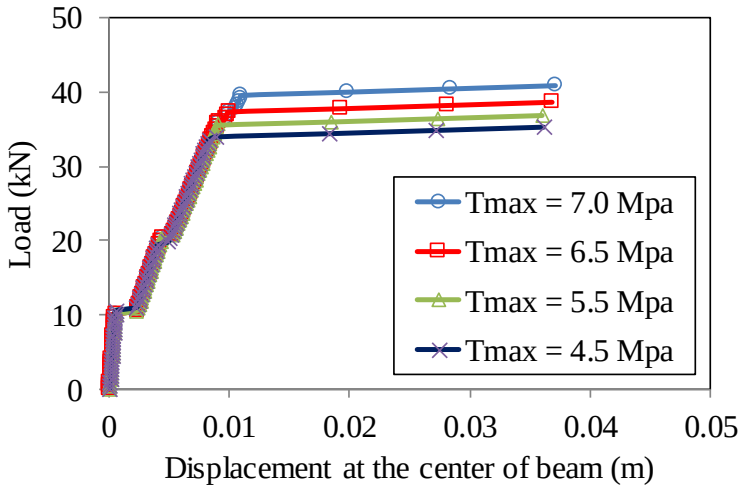

Fig. 16–Load-displacement relationship of the beam with various reduction of the adhesion forces between concrete and reinforcing bars

4.3 Effect of the corrosion time

We also conducted a series of experimental tests to investigate the influence of corrosive embedded times on the loading capacity of RC beams, as shown in Fig. 17. Three types of RC beam specimens with different corrosion times including one month, two months, and three months, were considered. After the precast 28-day period, the beams were moved to the accelerated corrosion process.

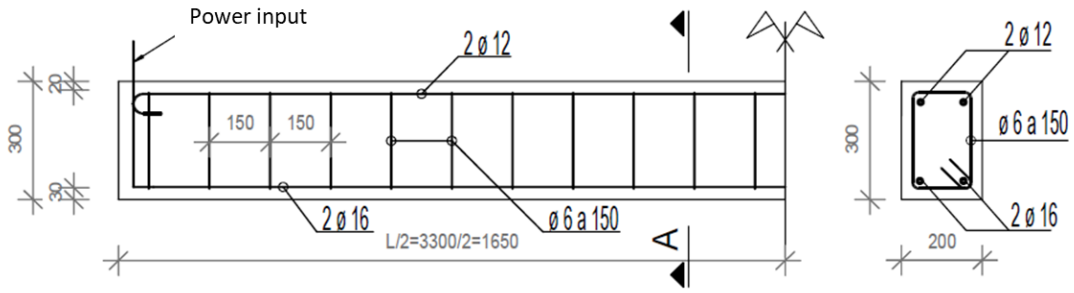

Fig. 17–Dimensions and details of RC beams for accelerated corrosion tests

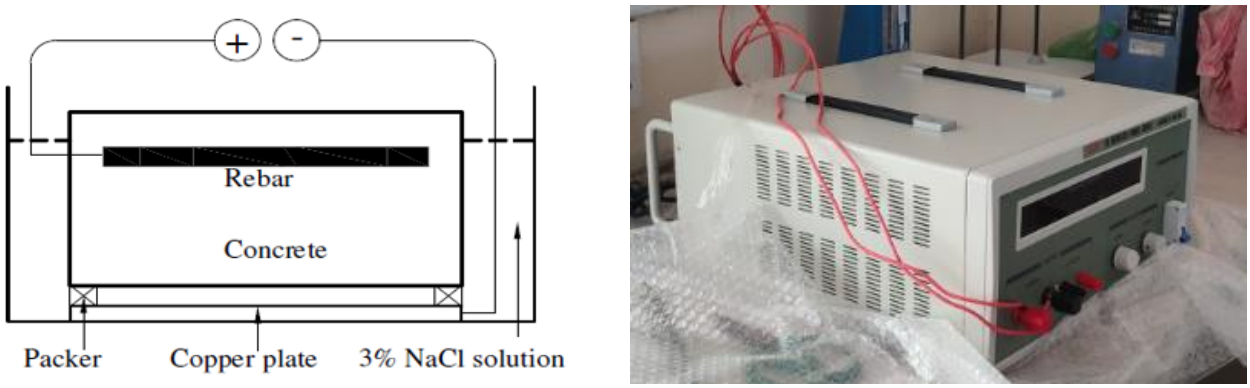

(a) The corrosion circuit (b) The direct current power used

Fig. 18–The accelerated corrosion test

Fig. 18(a) shows the accelerated corrosion test of the specimens. To perform this test, the bottom part of the beams was firstly embedded in a tank filled with 3.0% NaCl solution. Then, the corrosion process was implemented with the anode is the reinforcing bars, whereas the stainless-steel bar hanging on the surface is the cathode, as shown in Fig. 19. During the accelerated corrosion test, the direct current power type, QJ6030S (0~60V/0~30A), was applied for the corrosion current of each specimen (see Fig. 18(b)). It should be noted that an additional RC beam without corrosion effect is also constructed to make a comparison of the loading capacity.

The corroded beam specimens were thereafter imposing on the flexural tests after finishing the accelerated corrosion process, as shown in Fig. 20. To measure the deflection of the beams, the linear variable displacement transducers (LVDT) were attached at the middle and one-fourth beam locations. The strengths of tested RC beams are summarized in Table 3.

(a) Corrosion specimens (b) close-up image of the corroded beam

Fig. 19–RC beam for accelerated corrosion tests

Fig. 20–Experimental test setup of RC beams

Table 3 - Flexural strength of RC beams with different corrosion times

RC beams	No corrosion	1-month corrosion	2-month corrosion	3-month corrosion
Strength (kN)	110	71	59	40

5 Conclusion

In this study, a finite element (FE) model of corroded reinforced concrete beams was developed considering the reduction of the reinforcement diameter and adhesion force between concrete and reinforcing bars. The model, which was composed by three main components including concrete elements, rebar elements, and adhesion elements, was built based on the plane cross-section hypothesis. This FE model was then verified by an experimental study, highlighting the capability of the

numerical model in performing load-carrying evaluation of corroded RC beams. Also, the effects of diameter reduction and adhesion forces on the behaviour of the beams were assessed. Additionally, a series of experimental tests were performed to evaluate the influence of corrosion time on the strength of corroded RC beams. Following conclusions are drawn.

A FE program for analyzing RC beams under corrosion effects was developed. The proposed algorithm built for FE model provided accurate and reliable results in simulating calculations of corroded RC beams. The necessary number of elements in the numerical model was greatly reduced while the accuracy of the model was still ensured.

The diameter reduction of reinforcing bars has a significant influence on the stiffness and strength of the corroded RC beam. Meanwhile, the variation of adhesive force has no effect on the stiffness of the beam, however it has a pronounced influence on the strength of the beam.

The corrosion time has a significant effect on the strength of RC beams. Thus, it is important to consider the effect of embedded corrosion time on evaluation of the capacity of RC beams.

The proposed algorithm of FE model can be expanded to apply for other RC structural members such as columns and shear walls.

Acknowledgement

This study was supported by project number B2019-SPK-11, funded by the Ministry of Education and Training, Vietnam.

Conflicts of interest

The authors declare that they have no potential conflicts of interest in this paper.

REFERENCES

[1]- J. Rodriguez, L.M. Ortega, J. Casal, Load carrying capacity of concrete structures with corroded reinforcement. Constr. Build. Mater. 11(4) (1997) 239-248. doi:10.1016/S0950-0618(97)00043-3

[2]- T. Vidal, A. Castel, R. Francois, Analyzing crack width to predict corrosion in reinforced concrete. Cement Concrete Res. 34(1) (2004) 165-174. doi:10.1016/S0008-8846(03)00246-1

[3]- C. Lu, H. Tamai, Y. Sonoda, A Numerical Study on the Impact Resistant Capacity of RC Beams with Corroded Reinforcement. Procedia Engineer. 210 (2017) 341-348. doi:10.1016/j.proeng.2017.11.086

[4]- S.J. Han, H.E. Joo, S.H. Choi, I. Heo, K.S. Kim, S.Y. Seo, Experimental Study on Shear Capacity of Reinforced Concrete Beams with Corroded Longitudinal Reinforcement. Materials. 12(5) (2019) 837. doi:10.3390/ma12050837

[5]- G. Malumbela, M. Alexander, P. Moyo, Variation of steel loss and its effect on the ultimate flexural capacity of RC beams corroded and repaired under load. Constr. Build. Mater. 24(6) (2010) 1051-1059. doi:10.1016/j.conbuildmat.2009.11.012

[6]- W. Zhu, R. François, D. Coronelli, D. Cleland, Effect of corrosion of reinforcement on the mechanical behaviour of highly corroded RC beams. Eng. Struct. 56 (2013) 544-554. doi:10.1016/j.engstruct.2013.04.017

[7]- E.P. Kearsley, A. Joyce, Effect of corrosion products on bond strength and flexural behaviour of reinforced concrete slabs. J. the South African Inst. Civ. Eng. 56(2) (2014) 21-29. http://hdl.handle.net/2263/42418

[8]- I. Sæther, B. Sand, FEM simulations of reinforced concrete beams attacked by corrosion. ACI Struct. J. 39(2) (2012) 15-31.

[9]- K. Zandi Hanjari, Load-carrying capacity of damaged concrete structures, Master's thesis in Structural Engineering, Chalmers University of Technology, Gothenburg, 2008.

[10]- A. Shetty, K. Venkataramana, K.S.B. Narayan, Experimental and numerical investigation on flexural bond strength behavior of corroded NBS RC beam. Int. J. Adv. Struct. Eng. 7(3) (2015) 223-231. doi:10.1007/s40091-015-0093-6

[11]- P. Koteš, M. Brodnan, Numerical modeling of the reinforcement corrosion of RC T-beam. Engineer Mechan. 20(5) (2013) 389-399

[12]- D. Coronelli, P. Gambarova, Structural assessment of corroded reinforced concrete beams: modeling guidelines. J. Struct. Eng-ASCE. 130(8) (2004) 1214-1224. doi:10.1061/(ASCE)0733-9445(2004)130:8(1214)

[13]- H. Hussain, D. Miteva, Structural behavior of corroded reinforced concrete structures - A study based on detailed 3D FE analyses, Master's thesis in Structural Engineering, Chalmers University of Technology, Gothenburg, 2018.

[14]- I.M. Smith, D.V. Griffiths, L. Margetts, Programming the finite element method. John Wiley & Sons, Inc. Fifth Edition, 2013.

[15]- M.H. Scott, G.L. Fenves, F. McKenna, F.C. Filippou, Software patterns for nonlinear beam-column models. J. Struct. Eng. 134(4) (2008) 562-571. doi:10.1061/(ASCE)0733-9445(2008)134:4(562)

[16]- F. Li, Y. Yuan, Effects of corrosion on bond behavior between steel strand and concrete. Constr. Build. Mater. 38 (2013) 413-422. doi:10.1016/j.conbuildmat.2012.08.008

[17]- A. Shetty, I. Gogoi, K. Venkataramana, Effect of loss of bond strength due to corrosion in reinforced concrete members. Int. J. Earth Sci. 4 (2011) 879-884.

[18]- T.H. Nguyen, A.T. Le, D.D. Nguyen, Bending strength diagnosis for corroded reinforced concrete beams with attendance of deterministic, random and fuzzy parameters. J. Struct. Integ. Main. 5(3) (2020) 183-189. doi: 10.1080/24705314.2020.1765268